Charge-transfer cross sections for multiply charged ions colliding with gaseous targets at energies from 310 keV/amu to 8.5 MeV/amu

W. G. Graham,* K. H. Berkner, R. V. Pyle, A. S. Schlachter, J. W. Stearns, and J. A. Tanis†
Lawrence Berkeley Laboratory, University of California, Berkeley, California 94720
(Received 21 February 1984)

Electron-capture and electron-loss cross sections are reported for a large number of combinations of projectile species (C, Ar, Fe, Nb, and Pb), target gases (H_2, He, N_2, Ne, Ar, and Xe), projectile charge states (6+ to 59+), and energies (310 keV/amu to 8.5 MeV/amu). These measured cross sections are compared with published theoretical calculations and scaling rules.

I. INTRODUCTION

We report measurements of electron-capture and electron-loss cross sections for a wide range of highly charged ions with energies between 310 keV/amu and 8.5 MeV/amu, incident on gas targets. These measurements are used to evaluate recent theoretical calculations and empirical and semiempirical scaling rules in a charge state and energy range where few experimental measurements have been previously published.

The cross sections we have measured are $\sigma_{q,q-n}$ for the electron-capture process

$$X^{q+}+Y\rightarrow X^{(q-n)+}+Y^{m+}+(m-n)e$$

and $\sigma_{q,q+n}$ for the electron-loss process

$$X^{q+}+Y\rightarrow X^{(q+n)+}+Y^{m+}+(m+n)e\ .$$

The present measurements are primarily of single electron capture and single electron loss ($n=1$); some measurements of double electron capture and double electron loss ($n=2$) are also reported. Cross sections (Table I) have been measured for a large number of combinations of projectile species (C, Ar, Fe, Nb, and Pb), target gases (H_2, He, N_2, Ne, Ar, and Xe), projectile charge states (6 + to 59 +), and energies (310 keV/amu to 8.5 MeV/amu).

The present discussion is limited to projectiles heavier than C and energies greater than 300 keV/amu, i.e., the intermediate to high velocity regime, $v/v_0>3.5$, where v is the projectile velocity and v_0 is the Bohr velocity (2.2×10^8 cm/sec). We compare the present results with previous measurements reported for charge transfer with fast projectiles.

Much of the current theoretical work on charge transfer is for an atomic-hydrogen target. Experimental data for charge transfer of fast multiply charged ions in an H_2 target can be compared with theoretical calculations for an atomic-hydrogen target by use of approximate factors based on limited experimental results in H_2 and H targets. For target ionization[1] and projectile electron loss,[2] cross sections calculated for an atomic-hydrogen target can be multiplied by a factor of approximately 2 to compare with measured cross sections in molecular hydrogen. The use of such a factor for electron capture possibly is not justified,[3,4] hence the discussion of theoretical electron-capture cross sections will be restricted to rare-gas targets.

Electron-capture cross sections at the present intermediate to high velocities ($v/v_0>1$) have been calculated using both quantum-mechanical and classical techniques.[5] The present discussion will be limited to published calculations and scaling rules which can be applied directly to the present experimental collision partners. Although it is well-known[6] that the Oppenheimer-Brinkman-Kramers (OBK) approximation considerably overestimates the experimental cross sections, several authors have used the OBK approximation to estimate electron-capture cross sections or deduce scaling rules theoretically. Rule and Omidvar[7] have used the OBK approximation, modified by the empirical factor suggested by Nikolaev,[6] to calculate electron-capture cross sections in Ar targets. Tawara[8] has used similarly modified OBK calculations for a scaling rule for He targets. Chan and Eichler[9] have used the classical-trajectory eikonal approximation, which takes into account the interaction of the captured electron with both the target and the projectile nucleus, to calculate correction factors to be applied to cross sections obtained by the OBK method; these correction factors can be used for various projectile and target combinations. The full first Born approximation was used by Janev *et al.*[10] to deduce a scaling rule for electron-capture cross sections for multiply charged ion collisions with Ar.

Knudsen *et al.*[11] have used the classical model of Bohr and Lindhard[12] combined with the statistical first-order Lenz-Jensen atom model to calculate electron-capture cross sections in various gas targets; their calculations produced a target-Z scaling of electron-capture cross sections for different multiply charged ions. We determined in a previous paper[13] an empirical expression for the electron-capture cross sections for multiply charged iron ions in a molecular hydrogen target; we subsequently[4] found an empirical universal scaling rule for electron-capture cross sections for multiply charged ions in a variety of target gases.

In the case of electron loss the cross sections are predicted to have a broad maximum as a function of projectile energy. According to the theoretical work of Bohr and Lindhard,[12] this maximum is expected when the projectile velocity is slightly greater than the velocity of the

TABLE I. Electron-capture and electron-loss cross sections in units of 10^{-18} cm^2/atom (10^{-18} cm^2/molecule for H_2 and N_2 targets). Random standard uncertainties are ±5% unless otherwise indicated. Systematic uncertainties contribute an additional ±7% to absolute magnitudes, except for electron-capture cross sections for H_2 and He targets where systematic uncertainties add −7%, + 14% to absolute magnitudes.

Target	Projectile	Energy (MeV)	MeV/amu	Charge state	$\sigma_{q,q-1}$	$\sigma_{q,q-2}$	$\sigma_{q,q+1}$	$\sigma_{q,q+2}$
$(_1H)_2$	$_{18}Ar$	336	8.4	17			0.0052[c]	
$(_1H)_2$	$_{82}Pb$	970	4.66	59	0.46[c]		0.14[b]	
				58	0.44[a]	0.029[c]	0.143	
				57	0.48	0.023[b]	0.175	
				56	0.46[a]	0.023[b]	0.21[a]	
				55	0.39	0.017[d]	0.23[a]	
				54	0.38[a]	0.021[d]	0.25[a]	
				53	0.33[a]		0.34[a]	0.023[d]
				52	0.32	0.015[d]	0.35[a]	
				51	0.31	0.015[b]	0.43	
$(_1H)_2$	$_{41}Nb$	320	3.43	34	0.21	0.015[c]	0.040[b]	
				31	0.12		0.22	0.014[b]
				28	0.10	0.0037[b]	0.32	0.023[b]
$(_1H)_2$	$_6C$	13.7	1.14	6	0.17[d]			
		3.7	0.31	6	62			
$_2He$	$_{82}Pb$	970	4.66	54	0.89		0.28	
$_2He$	$_6C$	13.7	1.14	6	1.0			
		3.7	0.31	6	130			
$(_7N)_2$	$_{82}Pb$	970	4.66	54	88	9.0	3.2[a]	
$_{10}Ne$	$_{82}Pb$	970	4.66	54	48	10.3	1.8[c]	0.23[d]
	$_6C$	13.7	1.14	6	17.0			
$_{18}Ar$	$_{26}Fe$	470	8.4	26	6.0	1.3[a]		
				25	5.7	0.98		
	$_{18}Ar$	340	8.5	18	2.4[a]			
				17	2.4	0.15	0.25	
	$_{82}Pb$	970	4.66	54	83	21	2.5[d]	
	$_{41}Nb$	318	3.4	31	60	16	1.2[c]	
	$_{26}Fe$	190	3.4	25	45	9.8		
				24	43	9.4		
				23	39	8.0	0.34[b]	
	$_{18}Ar$	136	3.4	16	23	4.3		
	$_{26}Fe$	60	1.07	21	143	53		
				20	150	46[a]		
	$_6C$	13.7	1.14	6	33			
$_{54}Xe$	$_{82}Pb$	970	4.66	54	75	26[a]	3.9[a]	

[a] 10% uncertainty.
[b] 15% uncertainty.
[c] 20% uncertainty.
[d] 30% uncertainty.

electron about to be lost. The measurements presented here are for energies which are at or slightly below the energy of the predicted maximum for the present projectiles.

Electron-loss cross sections have been calculated using Bohr theory[4] and the Born approximation.[15–18] The Born approximation has been used by Dmitriev *et al.*,[15] Nikolaev *et al.*,[16] Gillespie,[17] and Shirai *et al.*[18] to calculate electron loss for hydrogenlike ions in various gas targets, while Rule and Omidvar[7] have used it to calculate electron-loss cross sections for Fe and O projectiles of various charge states in atomic hydrogen. The results of these various theoretical calculations and empirical scaling rules will be compared with the present experimental data.

II. EXPERIMENTAL APPROACH

A. Apparatus

The apparatus and experimental techniques used in the present measurements have been previously described in detail.[13,19] Ions of the desired energy, mass, and charge

state from the SuperHILAC accelerator at the Lawrence Berkeley Laboratory were selected, after passage through a foil, by momentum analysis and passed through a well-defined target region. The methods used to ensure correct charge-state identification and energy measurement are discussed in Ref. 13.

After passage through the target gas, the beam was charge-state analyzed using a spectrometer magnet. The charge-analyzed beams were detected by an array of five solid-state detectors. This allowed single and double electron-capture and electron-loss cross sections to be measured simultaneously. In some cases, when target ionization measurements were being made,[13,19] the detector array was replaced by a double Faraday cup, with which either $\sigma_{q,q-1}$ or $\sigma_{q,q+1}$ could be measured. Some cross sections were measured using both methods, and it was found that the measured cross sections agreed to within the estimated uncertainties.

The target-gas cell consisted of a differentially pumped chamber in which the pressure was measured with a capacitance manometer which had been calibrated with an oil manometer. At maximum target-gas-cell pressure the beam-line pressure in front of the gas cell was maintained at less than 1×10^{-4} Pa (1×10^{-6} Torr) to ensure that the charge-state purity of the incident beam was better than 99%. The magnetic spectrometer after the gas cell was maintained at pressures less than 3×10^{-4} Pa (2×10^{-6} Torr) to minimize charge transfer of the beam during charge-state analysis.

B. Data acquisition

Cross-section measurements were made for an incident charge state, after first determining that the detector count rates corresponding to each of the charge states was independent of small changes in the spectrometer magnetic field. Data were then accumulated to achieve better than 1% counting statistics for at least ten different target gas-cell pressures for each collision system. Beam attenuation was, in all cases, less than 10%. Least-squares fits of the $q\pm n$ fractions as a function of target thickness gave the cross sections $\sigma_{q,q\pm n}$. Corrections for beam attenuation and second-order processes were included in the analysis.[13]

C. Uncertainties

The random standard uncertainty in the cross sections was obtained from uncertainties in the least-squares fit (which averages the contributions from counting statistics, zero drift in the capacitance manometer, and correction for second-order processes) and from possible beam-energy drift during a sequence of measurements. The latter effect is estimated to contribute ±2% to the uncertainties in present measurements. The former contribution varies somewhat from measurement to measurement, depending on the magnitude of the effects mentioned. The random standard uncertainty is generally ±5%, but was as large as ±30% for a few measurements. The random standard uncertainty for each particular measurement is given in Table I.

Systematic uncertainties occur in the determination of the target thickness (calibration of the capacitance manometer and determination of the gas-cell length) and are estimated to be ±4%; in possible beam loss through scattering, estimated to be ±5%; and in possible impurities in the target gas. The effect of impurities will depend on the gas target; it is maximum for H_2 and He, for which the charge-transfer cross sections are small. Therefore, measurements with these gases were made before those in heavier targets, and care was taken to ensure that gas lines were not contaminated. In one sample of H_2 analyzed for impurities, 0.06% of N_2 was detected. From the data obtained at 4.66 MeV/amu with Pb^{54+} projectiles, we estimate impurities at this level could lead to a 1% overestimate of electron-loss cross sections and a 12% overestimate of electron-capture cross sections for the H_2 and He targets. The effects of similar impurity levels for the heavier targets would be negligible.

The combined systematic uncertainties are, therefore, estimated to be 7% for electron-capture and electron-loss cross sections in N_2, Ne, Ar, and Xe and for electron-loss cross sections in H_2 and He, while electron-capture cross sections in H_2 and He are estimated to have systematic uncertainties of −7% and +14%. The absolute standard uncertainty can be obtained by combining the random and systematic uncertainties in quadrature.

III. RESULTS AND DISCUSSION

All of the cross sections measured in this work are given in Table I. The cross sections for each of the charge changing processes will be discussed separately.

A. Single electron capture

Direct comparison of the present results for $\sigma_{q,q-1}$ with previous experimental measurements is difficult since there are few measurements reported for the energies used with the present projectiles. Measurements[20,21] for which direct comparison is possible are shown in Table II. In these three cases the present and previous measurements agree within the combined experimental uncertainties.

The present electron-capture cross sections show a dis-

TABLE II. Comparison of present single-electron-capture cross sections with those reported previously, in units of 10^{-18} cm^2/atom.

Target	Projectile	Energy (MeV/amu)	Present	Previous	Reference
$_2$He	$_6C^{6+}$	1.14	$1.00^{-0.09}_{+0.15}$	0.81±0.05	20
$_{18}$Ar	$_{26}Fe^{25+}$	8.4	5.7±0.5	5.0 ±1.0	21
$_{18}$Ar	$_{26}Fe^{26+}$	8.4	6.0±0.5	5.5 ±1.1	21

tinct dependence on the charge state q of the projectile, as expected. To quantify the charge-state dependence, we assume a simple power-law dependence and determine the exponent from a least-squares fit of the cross sections, without consideration of the relative uncertainties. The uncertainty in the exponent is taken to be the standard deviation obtained for the least-squares fit. In the case of Pb^{q+} projectiles ($q=51$ to 59) incident on H_2 the capture cross sections obtained at 4.66 MeV/amu show a $q^{3.2\pm0.6}$ dependence, while those obtained with Nb^{q+} projectiles ($q=28$, 31, and 34) incident on H_2 at 3.43 MeV/amu exhibit a $q^{3.8\pm1.7}$ dependence, in general agreement with the $q^{3.15}$ dependence we reported previously for Fe^{q+} projectiles.[13] These are the only projectiles for which sufficient data exist to establish a q dependence. Most theories for fully stripped ions predict a q^3 dependence in the intermediate velocity regime, going to q^5 in the limit of high velocities.[5]

The single-electron-capture cross sections (Table I) are presented in Fig. 1 using the reduced parameters $\tilde{\sigma}=\sigma Z_2^{1.8}/q^{0.5}$ and $\tilde{E}=E/(Z_2^{1.25}q^{0.7})$ from our empirical scaling rule for single electron capture,[4] where σ is the single-electron-capture cross section, Z_2 is the atomic number of the target gas, q is the projectile charge state, and E is the projectile energy in keV/amu. The reduced parameters were determined by a nonlinear least-squares fitting routine to our present and our previously reported single-electron-capture cross sections.[4]

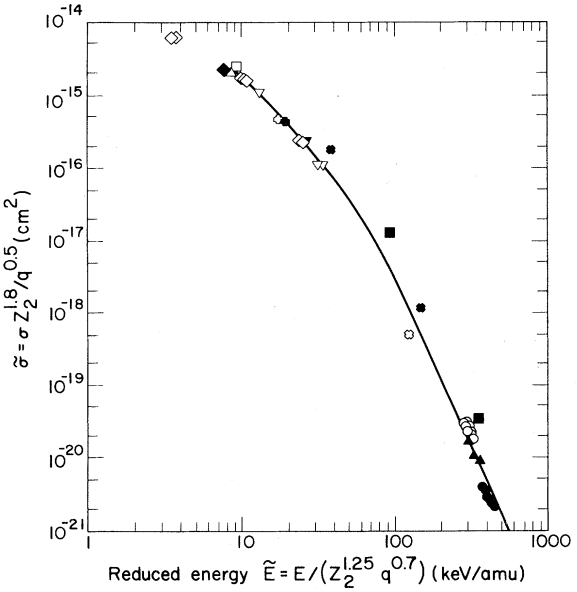

FIG. 1. Single-electron-capture cross sections for multiply charged ions incident on various gas targets plotted in terms of reduced parameters $\tilde{\sigma}=\sigma Z_2^{1.8}/q^{0.5}$ and $\tilde{E}=E/(Z_2^{1.25}q^{0.7})$ (Ref. 4). Symbols: C projectiles on H_2, ■; He, ✕; Ne, ✚; Ar, □. Ar projectiles on Ar, ∇. Fe projectiles on Ar, ◇. Nb projectiles on H_2, ▲; Ar △. Pb projectiles on H_2, ○; He, ⊠; N_2, ▼; Ne, ✣; Ar, ◆. Also shown: Fe projectiles on H_2 (Ref. 13), ●. The line represents the scaling-rule function (Ref. 4) described by Eq. (1) in the text. [Data for H_2 and N_2 are divided by two, and Z_2 values of 1 and 7, respectively, are used to obtain the reduced parameters (Ref. 4).]

The solid line in Fig. 1 represents the scaling relation reported in Ref. 4:

$$\tilde{\sigma}=\frac{1.1\times10^{-8}}{\tilde{E}^{4.8}}[1-\exp(0.037\tilde{E}^{2.2})]$$
$$\times[1-\exp(-2.44\times10^{-5}\tilde{E}^{2.6})]\,. \quad (1)$$

This empirical scaling rule contains no explicit dependence on the projectile atomic number Z_1. We have found that 70% of all the electron-capture cross sections measured by both the present authors and others, when plotted in these reduced parameters, lie within a factor of 2 of the curve described by Eq. (1).[4] However, within these limits, there are some features which suggest a projectile species dependence. The most obvious feature is the C^{6+} cross sections in H_2 and He which lie above the scaling-rule line. Less obvious, on the compressed scale of Fig. 1, is the tendency for Pb^{q+} cross section in H_2 to lie above, Nb^{q+} cross sections to lie close to, and our previous Fe^{q+} cross sections[13] to lie below, the scaling rule line.

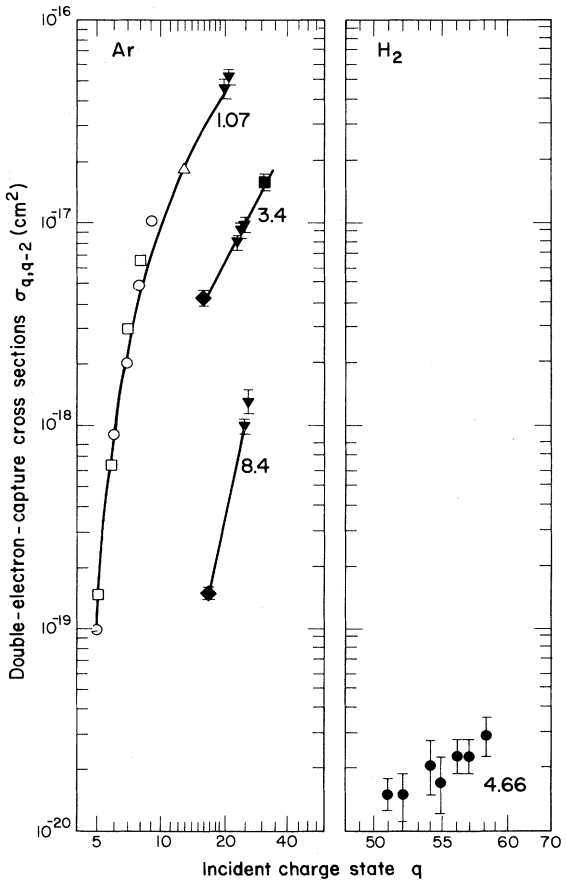

FIG. 2. Double-electron-capture cross sections $\sigma_{q,q-2}$ vs q in H_2 and Ar. Present experimental results: ◆, Ar^{q+} (3.4 and 8.4 MeV/amu); ▼, Fe^{q+} (1.07 and 8.4 MeV/amu); ■, Nb^{q+} (3.4 MeV/amu); ●, Pb^{q+} (4.66 MeV/amu). Previous experimental results: □, O^{q+} (1.1 MeV/amu) Ref. 22; ○, F^{q+} (1.1 MeV/amu) Ref. 23; △, Cl^{13+} (1.0 MeV/amu) Ref. 24. Lines are to guide the eye. The numbers represent the approximate energy in MeV/amu.

B. Double electron capture

Double-electron-capture cross sections for Pb^{q+} ($q=51$ to 58) at 4.66 MeV/amu in H_2 are shown in Fig. 2 as a function of incident charge state. The double-electron-capture cross sections are generally about a factor of 20 lower than those for single electron capture. The double-electron-capture cross sections show a $q^{(6\pm2)}$ dependence, compared to the $q^{(3.2\pm0.6)}$ dependence found for the single-electron-capture cross sections. The double-electron-capture cross sections we report here are apparent cross sections; transfer ionization (e.g., double electron capture into a doubly excited state followed by autoionization) would appear in the single-electron-capture channel.

We also present in Fig. 2 double-electron-capture cross sections (Table I) for the various multiply charged ions in Ar (closed symbols) as a function of incident charge state. The double-electron-capture cross sections are about a factor of 4 less than those for single electron capture in Ar. Also shown (open symbols) are previously reported double-electron-capture cross-section measurements for F^{q+} and O^{q+} at 1.1 MeV/amu (Refs. 22 and 23) and Cl^{13+} at 1.0 MeV/amu.[24] The double-electron-capture cross sections for lower-q projectiles appear to have a steeper charge-state dependence than those for the higher-q projectiles reported in Table I.

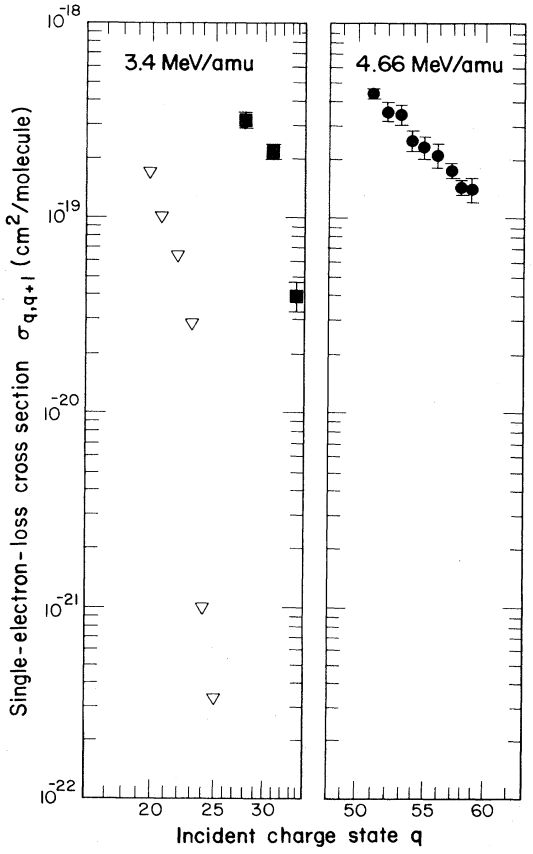

FIG. 3. Single-electron-loss cross sections $\sigma_{q,q+1}$ vs q in H_2. Present experimental results: ■, Nb^{q+}; ●, Pb^{q+}. Previous experimental results: ▽, Fe^{q+} (Ref. 13).

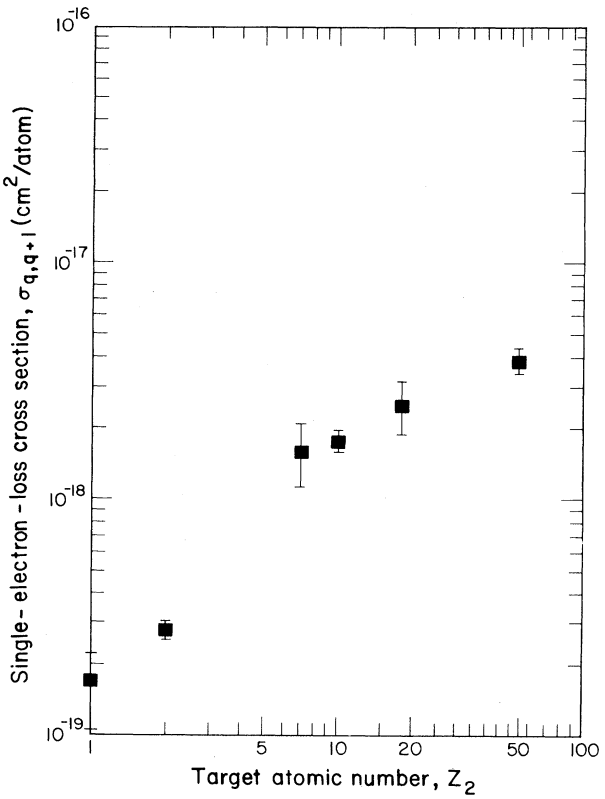

FIG. 4. Single-electron-loss $\sigma_{q,q+1}$ cross sections as a function of the atomic number of the target gas for incident 4.66 MeV/amu Pb^{54+}. (The results for H_2 and N_2 are divided by 2.)

C. Single electron loss

Single-electron-loss cross sections measured in the present work for H_2 are shown in Fig. 3. The cross sections exhibit a strong charge-state and projectile-species dependence.

Our previously reported measurements[13,25] for Fe^{q+} in H_2 are also shown in Fig. 3. The Fe^{q+} measurements[13,25] with $q>10$ showed a q^{-9} to q^{-10} dependence, while the present data show a $q^{(-8.1\pm0.4)}$ dependence for Pb^{q+} and about q^{-11} for Nb^{q+}.

The target-gas dependence of electron-loss cross sections for 4.66 MeV/amu Pb^{54+} in various gas targets is presented in Fig. 4. The cross sections are seen to increase monotonically with the atomic number of the target gas.

D. Double electron loss

A few measurements of double-electron-loss cross sections are presented in Table I. There are too few data to draw any conclusions, except that they are generally an order of magnitude less than the single-electron-loss cross sections for the same ion.

IV. COMPARISON WITH THEORY

A. Electron capture

The present measured single-electron-capture cross sections are compared with published theoretical calculations

TABLE III. Comparison of present single-electron-capture cross sections, previously published theoretical calculations, and cross sections obtained from theoretically derived scaling rules. Cross sections are in units of 10^{-18} cm^2/atom.

Target	Projectile	Charge state	Energy (MeV/amu)	Present Measurement	Theoretical cross sections				
					Ref. 11	Ref. 7	Ref. 10	Ref. 9	Ref. 8
$_2$He	$_6$C	6	0.310	130^{-10}_{+20}	49			174	180
			1.14	$1.0^{-0.08}_{+0.14}$	0.94			1.11	0.43
	$_{82}$Pb	54	4.66	$0.89^{-0.08}_{+0.13}$	6.8			1.62	
$_{18}$Ar	$_6$C	6	1.14	33 ±2.8	19		20		
	$_{18}$Ar	18	8.4	2.4±0.3	1.8	5.8	2.3		
		17	8.4	2.4±0.2	1.5	5.0	1.9		
		16	3.4	23 ±2	12	54	28		
	$_{26}$Fe	26	8.4	6.0±0.5	3.4	16.2	10		
		25	8.4	5.7±0.5	4.7	14.4	9.4		
		25	3.4	45±4	43	257	110		
		24	3.4	43±4	42	191	98		
		23	3.4	39±35	40	167	87		
		21	1.1	143±12	420	3420	710		
		20	1.1	150±13	400	2940	640		
	$_{41}$Nb	31	3.4	60±5	67		190		
	$_{82}$Pb	54	4.66	83±7	140		875		

in Table III. The modified OBK calculations of Chan and Eichler[9] give good agreement with the present measurements for C^{6+} in He, but the agreement is poorer for 4.66 MeV/amu Pb^{54+} in He. The cross sections calculated by Rule and Omidvar,[7] also using a modified OBK approximation, overestimate the present measurements in Ar.

Several single-electron-capture scaling rules based on theory have been published as mentioned previously. The present measurements are compared in Table III with cross sections obtained from these scaling rules. The cross sections obtained from the scaling rule of Knudsen *et al.*,[11] based on the Bohr and Lindhard[12] model, are generally in reasonable agreement with the present measurements. Those obtained from the scaling rule of Tawara,[8] based on a modified OBK approximation, show agreement only at the lowest energy. The cross sections obtained from the first-Born-approximation scaling rule of Janev *et al.*,[10] which are applicable to fully stripped ions, show good agreement with the measured cross sections for C^{6+} and $Ar^{16+,17+,18+}$ projectiles, but the cross sections for other projectiles and charge states are overestimated.

TABLE IV. Comparison of present single-electron-loss cross section for $Ar^{17+} + H_2$, at 8.4 MeV/amu, with theoretical calculations. The theoretical calculations are for atomic hydrogen and are multiplied by 2 for comparison. Cross sections are in units of 10^{-21} cm^2/molecule.

Experiment	Theory	Reference
5.2±1.1		
	6.0	15
	6.0	16
	2.9	17
	7.2	18

B. Electron loss

Theoretical calculations which can be compared with the present measurements have generally been restricted to hydrogenlike ions.[15–18] These calculations are compared in Table IV with our measurements for Ar^{17+} in H_2. The calculations, all based on the Born approximation, are for atomic-hydrogen targets, and have been multiplied by two for comparison. The agreement among the experimental cross sections and most of the calculated values is good. Born calculations for non-hydrogen-like ions generally underestimate the present experimental results by more than an order of magnitude.

The Bohr theory,[26] which is valid for higher energies than those used in the present work, is found to considerably overestimate the single-electron-loss cross sections of Table I. Knudsen *et al.*[27] have shown that, for heavy gas targets at lower energies and charge states, the Bohr theory gives quite good target-gas dependence. For targets heavier than nitrogen, the present measurements for 4.66 MeV/amu Pb^{54+} show a $Z_2^{0.47\pm0.02}$ dependence, where Z_2 is the atomic number of the target. The Bohr theory[26] predicts a $Z_2^{0.67}$ dependence at higher energies.

V. CONCLUSIONS

We have measured electron-capture and electron-loss cross sections for a variety of fast multiply charged ions in a number of gas targets. Measured single-electron-capture cross sections were found to be in reasonable agreement with the modified OBK calculations of Chan and Eichler[9] and the classical Bohr and Lindhard calculations of Knudsen *et al.*[11] Double-electron-capture cross sections are substantially lower than single-electron-capture cross sections, by a factor of ~20 in H_2 targets and a factor of ~4 in Ar targets. The double-electron-capture cross sections also exhibit a steeper charge-state

dependence than the single-electron-capture cross sections.

Electron-loss cross sections show a strong charge-state and projectile-species dependence. A q^{-8} dependence is found in the present energy regime, which is consistent with that which we reported previously for Fe^{q+} projectiles.[13,15]

Theoretical calculations[15–18] of electron-loss cross sections for hydrogenlike ions based on the Born approximation are generally in good agreement with our experimental measurements for Ar^{17+} in H_2, but underestimate the cross sections for other projectiles.

ACKNOWLEDGMENTS

We would like to thank Dr. P. J. Schneider and Dr. K. R. Stalder for assistance with some of these experiments. This work was supported by the Director, Office of Energy Research, Office of Fusion Energy, Applied Plasma Physics Division of the U.S. Department of Energy under Contract No. DE-AC03-76SF00098. During the final stages of this work, one of us (W.G.G.) received support from the North Atlantic Treaty Organization (NATO) Research Grants Program (Grant No. 1910).

*Present address: The New University of Ulster, Coleraine, Northern Ireland.

†Present address: Western Michigan University, Kalamazoo, MI 49008.

[1]M. B. Shah and H. B. Gilbody, J. Phys. B **15**, 3441 (1982).

[2]T. V. Goffe, M. B. Shah, and H. B. Gilbody, J. Phys. B **12**, 3763 (1979).

[3]H. Knudsen, H. K. Haugen, and P. Hvelplund, Phys. Rev. A **24**, 2287 (1981).

[4]A. S. Schlachter, J. W. Stearns, W. G. Graham, K. H. Berkner, R. V. Pyle, and J. A. Tanis, Phys. Rev. A **27**, 3372 (1983).

[5]D. S. F. Crouthers and N. R. Todd, J. Phys. B **13**, 2277 (1980).

[6]V. S. Nikolaev, Zh. Eksp. Teor. Fiz. **51**, 1263 (1966) [Sov. Phys.—JETP **24**, 847 (1967)].

[7]D. W. Rule and K. Omidvar, Astrophys. J. **229**, 1198 (1979).

[8]H. Tawara, Phys. Lett. **71A**, 208 (1979).

[9]F. T. Chan and J. Eichler, Phys. Rev. A **20**, 1841 (1979).

[10]R. K. Janev, L. P. Presnyakov, and V. P. Shevelko, Phys. Lett. **76A**, 121 (1980).

[11]H. Knudsen, H. K. Haugen, and P. Hvelplund, Phys. Rev. A. **23**, 597 (1981).

[12]N. Bohr and J. Lindhard, K. Dan. Vidensk. Selsk. Mat.-Fys. Medd. **28**, No. 7 (1954).

[13]K. H. Berkner, W. G. Graham, R. V. Pyle, A. S. Schlachter, and J. W. Stearns, Phys. Rev. A **23**, 2891 (1981).

[14]H. Knudsen, L. H. Andersen, H. K. Haugen, and P. Hvelplund, Phys. Scr. **26**, 132 (1982).

[15]I. S. Dmitriev, Ya. M. Zhileikin, and V. S. Nikolaev, Zh. Eksp. Teor. Fiz. **49**, 500 (1965) [Sov. Phys.—JETP **22**, 352 (1966)].

[16]V. S. Nikolaev, V. S. Senashenko, and V. Yu. Shafer, J. Phys. B **6**, 1779 (1973).

[17]G. Gillespie (private communication).

[18]T. Shirai, K. Igauchi, and T. Watanabe, J. Phys. Soc. Jpn. **42**, 238 (1977).

[19]A. S. Schlachter, K. H. Berkner, W. G. Graham, R. V. Pyle, P. J. Schneider, K. R. Stalder, J. W. Stearns, J. A. Tanis, and R. E. Olson, Phys. Rev. A **23**, 2331 (1981).

[20]T. R. Dillingham, J. R. MacDonald, and P. Richard, Phys. Rev. A **24**, 1237 (1981).

[21]J. Alonso, D. Dietrich, and H. Gould, IEEE Trans. Nucl. Sci. **NS-26**, 3686 (1979).

[22]J. R. MacDonald and F. W. Martin, Phys. Rev. A **4**, 1965 (1971).

[23]S. M. Ferguson, J. R. MacDonald, T. Chiao, L. D. Ellsworth, and S. A. Savoy, Phys. Rev. A **8**, 2417 (1973).

[24]B. Main [See H. D. Betz, Rev. Mod. Phys. **44**, 465 (1972)].

[25]K. H. Berkner, W. G. Graham, R. V. Pyle, A. S. Schlachter, and J. W. Stearns, Phys. Lett. **62A**, 407 (1977).

[26]N. Bohr, K. Dan. Vidensk. Selsk. Mat.-Fys. Med. **18**, No. 8 (1948).

[27]H. Knudsen, C. D. Moak, C. M. Jones, P. D. Miller, R. O. Sayer, G. D. Alton and L. B. Bridwell, Phys. Rev. A **19**, 1029 (1979).